prosthesis

MDPI

Article

Efficacy of Atmospheric Pressure Plasma Jet-Induced Surface Treatment on Wettability, Surface Topography, and Shear Bond Strength of Ceramic Surfaces for CAD-On Assembly

Haidar Alalawi [1,*], Ziyad Al Mutairi [2], Omar Al Abbasi [2], Fatima Al Dossary [2], Manayer Husain [2], Faleh Al Ghubari [2], Sultan Akhtar [3] and Moamen A. Abdalla [1]

[1] Department of Substitutive Dental Sciences, College of Dentistry, Imam Abdulrahman Bin Faisal University, P.O. Box 1982, Dammam 31441, Saudi Arabia; maabdalla@iau.edu.sa
[2] College of Dentistry, Imam Abdulrahman Bin Faisal University, Dammam 31441, Saudi Arabia; 2160006693@iau.edu.sa (Z.A.M.); 2140004705@iau.edu.sa (O.A.A.); 2160006890@iau.edu.sa (F.A.D.); 2160006271@iau.edu.sa (M.H.); 2160004633@iau.edu.sa (F.A.G.)
[3] Department of Biophysics, Institute for Research and Medical Consultations (IRMC), Imam Abdulrahman Bin Faisal University, Dammam 31441, Saudi Arabia; suakhtar@iau.edu.sa
* Correspondence: haalalawi@iau.edu.sa

Abstract: This study evaluated the effectiveness of atmospheric pressure plasma jet (APPJ) treatment on the surface characteristics and bond strength of zirconia and lithium disilicate ceramics for CAD-on restorations. A total of 70 cylindrical-shaped specimens of lithium disilicate and 70 disc-shaped specimens of Y-TZP zirconia were machined, thermally processed, surface-treated, and then resin-bonded. The specimens were grouped according to the following surface treatments: no surface treatment, sandblasting, plasma, sandblasting followed by plasma, sandblasting followed by universal adhesive, plasma followed by universal adhesive, and sandblasting and plasma treatment followed by universal adhesive. The treated surfaces were subjected to a wettability assessment via contact angle measurement and a topography assessment using scanning electron microscopy (SEM). The cemented assembly was subjected to shear bond strength testing with a universal testing machine, and the results were imported to SPSS 23.0 for statistical analysis. The results show that APPJ treatment induced a significantly low contact angle for both ceramics with no surface alteration upon scanning. Moreover, APPJ treatment produced a bonded assembly with a shear bond strength comparable to sandblasting. In conclusion, APPJ treatment should be considered an efficient surface treatment with a non-destructive nature that surpasses sandblasting with the provision of a high shear bond strength between CAD-on ceramics.

Keywords: plasma jet; ceramic surface treatment; CAD-on; zirconia; lithium disilicate; universal adhesive

check for updates

Citation: Alalawi, H.; Al Mutairi, Z.; Al Abbasi, O.; Al Dossary, F.; Husain, M.; Al Ghubari, F.; Akhtar, S.; Abdalla, M.A. Efficacy of Atmospheric Pressure Plasma Jet-Induced Surface Treatment on Wettability, Surface Topography, and Shear Bond Strength of Ceramic Surfaces for CAD-On Assembly. *Prosthesis* **2024**, *6*, 1228–1239. https://doi.org/10.3390/prosthesis6050088

Academic Editors: João Paulo Mendes Tribst and Rafaela Oliveira Pilecco

Received: 5 September 2024
Revised: 28 September 2024
Accepted: 1 October 2024
Published: 16 October 2024

Copyright: © 2024 by the authors. Licensee MDPI, Basel, Switzerland. This article is an open access article distributed under the terms and conditions of the Creative Commons Attribution (CC BY) license (https://creativecommons.org/licenses/by/4.0/).

1. Introduction

Plasma implementation has been surging in popularity within many related medical and dental fields. The application of plasma has two approaches: the therapeutic approach for vital tissues or the surface treatment of restorative and prosthetic materials. The latter application is intended for surface modification along with bioactive coating, which is used in implant manufacturing or surface modification to aid in enhanced interfacial bonding [1]. When the aim is to join different substrates, it is crucial to allow for complete flow of the adhesive over the adherent surfaces. Hydrophilic surfaces are difficult to completely wet, which limits the spread of the adhesive layer and, in turn, may result in interfacial void formation or improper interaction with the adherent interface. As a consequence, the resultant interface will be vulnerable to debonding and failure over time. Ceramic surfaces are hydrophobic in nature and thus require further surface treatment before bonding. This treatment is a deliberate surface modification aimed at increasing the surface

energy of the hydrophobic surface, decontaminating the interface, and providing a high surface area free of shallow micro-irregularities [2]. In studying the bonding mechanism, the initiation of reactive groups on the material surface is essential to attain a wettable surface and successful bonding. Inertness and hydrophilicity properties, such as those found in zirconia, demonstrate poor bonding, which has been attributed to an extreme decrease in the reactive (OH) groups that are essential for subsequent bonding [2,3]. Surface modification is eventually required for all ceramic types, such as glass ceramics [4]. Plasma surface treatment acts by shooting ionized particles onto the target surface to create the ideal microenvironment for improved surface energy and wettability [5,6]. This process results in the production of reactive species or groups on the treated surface without alteration of its structure, namely OH, O_3, H_2O_2, and NO [7], coupled with cleaning action [8]. Plasma is generated in one of the following two forms: thermal plasma [9] or cold plasma [10]. The cold (non-thermal) atmospheric pressure plasma method, abbreviated as CAPP [11] or NTAPP [1], has the marked characteristic of target preservation, which surpasses the other plasma types. This target preservation characteristic is achieved by preventing overheating by maintaining the temperature relatively within the range of the room temperature. Such characteristics are important for applications in living tissues and materials susceptible to thermal deterioration [1,12]. Other favorable features of the NTAPP method were evidenced by the simplicity of plasma generation, such as its low cost, short application time, and relative ease of implementation [11,13,14]. Plasma can be generated under two atmospheric conditions: low atmospheric pressure and atmospheric pressure. A carrier gas, such as argon, helium, nitrogen, or oxygen, is essential in plasma applications [11]. There are numerous processes that can be utilized in the production of the cold (non-thermal) atmospheric pressure plasma method, such as dielectric barrier discharge, corona discharge, gliding arc discharge, and plasma jet. Moreover, various types of plasma applications with different parameters and gas atmospheres have been investigated with mandatory in-lab preparation [15,16].

Generally, handheld plasma devices known as atmospheric pressure plasma jets (APPJs) have the advantage of simplified application and ease of usage within the in-office clinical setting for the delivery of the cold (non-thermal) atmospheric pressure plasma method due to the exclusion of the vacuum element surrounding the reactor. These devices have the option of working within ambient air, without the need for a carrier gas [11]. Compact devices such as plasma pens, needles, torches, or brushes all fall under the category of APPJs. Plasma generated using a Piezobrush® PZ3 is considered a type of APPJ and is referred to as piezoelectric direct discharge (PDD) because it utilizes a piezoelectric transformer with resultant high-voltage AC power [17–19].

The joining of two machinable ceramic interfaces is proposed under the CAD-on concept. This process is carried out via an integrated virtual design of the substructure framework and the veneering structure, followed by milling. The introduction of the CAD-on technique gave rise to the term tri-layer [20] or multilayer [21,22]; the latter term is more common in the literature. The CAD-on was proposed to render the fabrication process totally digitally driven and to overcome the inherent chipping of conventional porcelain veneering [23,24]. Digital incorporation of the CAD-on approach concept allowed for more consistent and standardized fabrication of veneering with fewer firing cycles and, in turn, less construction time compared with lengthy hand-layering techniques [23,25]. The CAD-on milled structure is joined to the underlying framework via either an intervening heat-treated layer of fusion glass–ceramic or resin cementation [26]. The advantages of the simple technique of joining CAD-on structures with resin cementation have been discussed in the literature [27–29]. A feldspathic-based machinable ceramic [22] has been proposed for CAD-on veneering, while high-strength glass ceramics such as lithium disilicate have also been implemented with advantageous strength properties [30,31]. Resin-based machinable ceramics could also be used, but without further heat treatment [32]. Another advantageous aspect of the CAD-on concept is its consideration for the intraoral repair of chipped or

delaminated fixed dental prostheses [33]. Generally, intraoral repair is undertaken to overcome the shortcomings of chipped restoration, without further replacement [34,35].

One of the most detrimental factors for ceramic bonding is the application of a compatible surface treatment prior to joining the different substrates. In turn, several surface treatments have been elaborated and/or combined together for the sake of creating strong and stable bonded interfaces [36]. Ideally, the adherent surface should be decontaminated and/or treated to provoke free surface energy. The boosting of surface energy has been correlated with enhanced wettability, and hence, results in low contact angle values [37,38]. In broad terms, air-borne particle abrasion has been routinely incorporated with various surface treatments of either acid-resistant or acid-sensitive ceramics [39,40]. Due to the nature of polycrystalline zirconia, the further application of functional monomers, mainly Methacryloyloxydecyl Dihydrogen Phosphate (MDP), has been recommended. In the case of decontaminated silica-based ceramics, a silane coupling agent should be applied prior to resin cementation [41,42]. Universal adhesives have been proposed for the simplification of bonding procedures, on either a tooth or a ceramic substrate. In a study of ceramic substrates, a universal adhesive incorporating MDP and silane coupling agent was used to promote bonding between resin cement and polycrystalline ceramics or silica-based ceramics [43].

The decontamination procedure is performed using acid etching or sandblasting. This procedure results in the creation of micro-irregularities along with an increase in the surface area, which is favored for optimum bonding. Such micro-irregularities are evidenced by the increase in the surface roughness of the treated surface or prominent changes in the surface topography upon SEM scanning. On the other hand, an immensely roughened surface could adversely affect the bond strength, as in the prolonged etching of glass ceramics or uncontrolled abrasion of polycrystalline ceramics [44]. Significant disagreement [45,46] has been reported in the literature regarding sandblasting of the zirconia interface, with some results demonstrating stress-induced phase transition and tetragonal–monoclinic transformation. Despite the resultant satisfactory bond strength and high surface energy achieved with sandblasting, a continuous search for other alternatives is required to avoid the possible resultant weak phase transition [47,48].

In this study, in an attempt to analyze failures of bonded interfaces between prosthetic substrates and within a simulated in vitro environment, shear bond strength, as indicative of the bonding quality, was investigated.

The objective of this study was to evaluate the effect of plasma applied via APPJ devices as a surface treatment (separately or combined) for zirconia and lithium disilicate. A wettability assessment and surface topography scanning of the ceramic surfaces were carried out and the shear bond strength of the bonded interface mimicking CAD-on layers was measured. It was hypothesized that plasma surface treatment via APPJ devices—applied separately or combined with other surface treatments—would not affect the wettability and surface topography of treated surfaces and would not provide an acceptable shear bond strength for ceramic bonding.

2. Materials and Methods

In this in vitro study, two types of machinable ceramic materials, zirconia and lithium disilicate, were used to assess the impact of APPJ surface treatment, both separately and combined with other treatments. An initial power analysis was performed using a two-tailed test to assess the difference between the two independent group means, a medium effect size (d = 0.50) and an alpha of 0.05. The results demonstrated that a power of 0.80 required a total sample of 10 specimens for each group. A total of 70 disc-shaped zirconia specimens (Copran® Zri, White Peaks, Essen, Germany) and 70 cylindrical-shaped lithium disilicate glass–ceramic specimens (IPS e.max CAD, Ivoclar Vivadent, Schaan, Liechtenstein) were used in this study. The materials used, their composition, and their manufacturer information are described in Table 1.

Table 1. Brand, composition & manufacturers of the materials used in this study.

Material/Type	Composition (Manufacturers' Data)	Manufacturer
Copran® Zri | (ZR) Group	Y_2O_3: 4.5–5.35%, Al_2O_3: 0.15–0.35%, Iron hydroxide3: 0–0.01%, Other Oxides: 0–0.06%	White Peaks, Essen, Germany
IPS e.max CAD (LDS) Group	SiO_2: 57.0–80.0, Li_2O: 11.0–19.0, K_2O: 0.0–13.0, P_2O_5: 0.0–11.0, ZrO_2: 0.0–8.0, ZnO: 0.0–8.0, Other and colouring oxides: 0.0–12.0	Ivoclar Vivadent, Schaan, Liechtenstein
Maxcem Elite™ Self-Etch/Self-Adhesive Dual Cure Resin Cement.	Hazardous Ingredients: Uncured Methacrylate Ester Monomers. Other ingredients: Non-hazardous inert mineral fillers, Ytterbium Fluoride, activators, stabilizers, and colorants.	Kerr, Brea, CA, USA
3M™ Single Bond Universal Adhesive	MDP phosphate Monomer, Dimethacrylate resins, HEMA, Vitrebond Copolymer, Filler, Ethanol, Water, Initiators, Silane	3M, Saint Paul, MN, USA

2.1. Specimen's Preparation

The zirconia specimens (Copran® Zri) were trephined out of a large blank (98 × 18) to obtain a cylindrical structure with a 10 mm diameter. Then, using a precision saw (BUEHLER Isomet-5000), each zirconia cylinder was sliced to create disc-shaped specimens measuring 2 mm thick. Cutting was carried out under running water with a blade speed of 1200 rpm, a blade thickness of 0.5 mm, and a load of 100 g. To eliminate the extra thickness of the discs, a fine-grit sandpaper disc fitted on a polishing machine (AutoMet250, Buehler Ltd., Lake Bluff, IL, USA) was utilized. Lithium disilicate glass–ceramic (IPS e.max CAD, Ivoclar Vivadent) was trephined out of a C 14 block to obtain cylinder-shaped specimens, measuring 5 mm in diameter and 4 mm in height, and then prepared in the same manner as the previous specimens. The specimens were prepared according to the shear bond ISO standard (ISO 29022: 2013 Dentistry–Adhesion-Notched- edge shear bond strength Test) [49].

The specimens from each ceramic material (N = 70) were further divided into seven groups based on the surface treatment used, as shown in Figure 1, with n = 10 for each intended surface treatment. The control (C) group received no surface treatment.

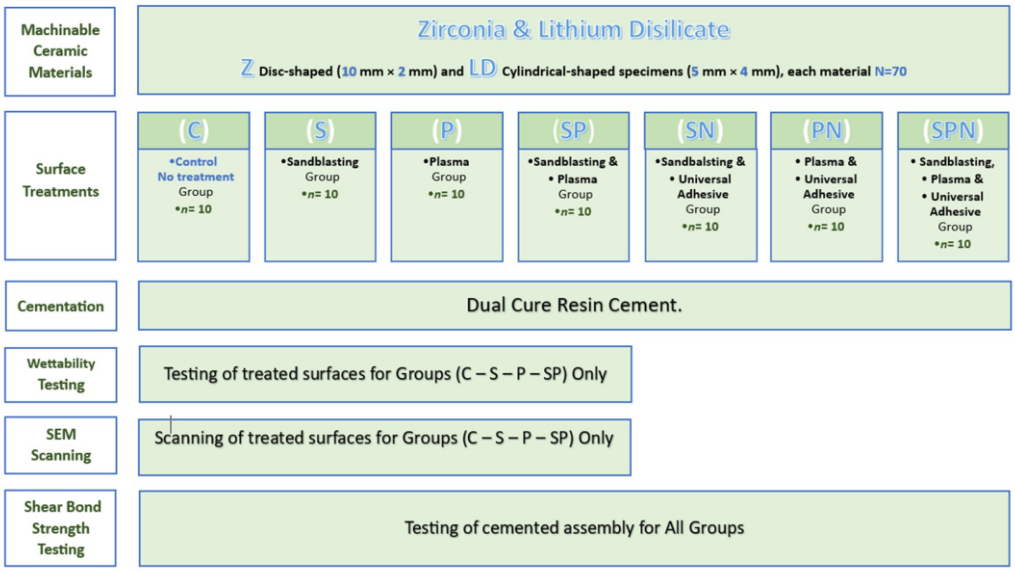


Figure 1. Testing setup chart and specimen grouping.

2.2. Specimens Surface Treatments

Sandblasting was conducted using 50 µm Aluminum Oxide (Al_2O_3 particles) at a 90° angle for 10 s at a 15 mm distance under 2 bar pressure. The plasma surface treatment was generated and applied via a handheld APPJ (Piezobrush PZ3, Relyon plasma, Regensburg, Germany) for 30 s at a 5 mm distance with 80% of the power. The plasma parameters and device used are presented in Table 2.

Table 2. Plasma Parameters.

Plasma Type	Type of Delivery Device Power	Model	Gas Medium	Duration	Distance to the Target	Power of Device
APPJ	Piezoelectric direct discharge	(Piezobrush PZ3, Relyon plasma, Regensburg, Germany)	Ambient Air	30 s	5 mm	80%

In terms of adhesive application, a disposable micro-brush was used to coat the zirconia surfaces with the silane and MDP-containing universal adhesive (3M Single Bond Universal Adhesive). Air thinning of the adhesive was performed using a triple syringe connected to a dental unit at a pressure of 40–50 psi and approximately 10 mm from the zirconia surface until there was no movement of the adhesive. Light curing was performed for 20 s perpendicular to the zirconia surface (Dentsply QHL75 Dental Curing Light, Dentsply Sirona USA, Charlotte, NC, USA). The sequence of surface treatments in multiple combinations was conducted in the order presented in Figure 1. Each cylindrical-shaped specimen of the lithium disilicate ceramic was cemented over the disc-shaped specimens of the zirconia ceramic after the application of the predetermined surface treatment. The cementation process of the lithium disilicate cylinder on the zirconia disc was conducted using Self-Etch/Self-Adhesive Dual Cure Resin Cement (Maxcem Elite) immediately after the application of the designated surface treatment. A standardized load of 5 Kg was used to hold the specimens for 15 min until the cement was set. The final assembly that was mounted in the testing machine is illustrated in Figure 2.

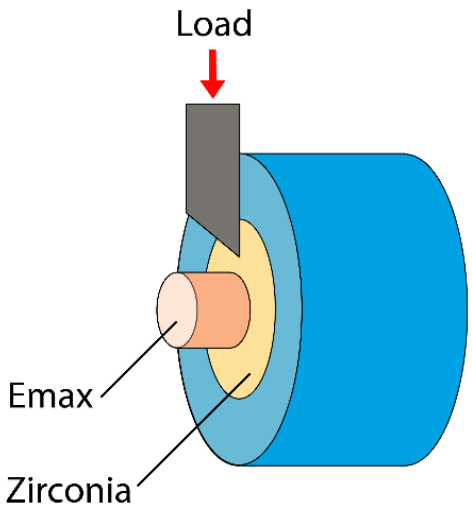


Figure 2. Specimen assembly.

2.3. Specimens Testing

2.3.1. Shear Bond Strength

The shear bond strength test was carried out according to ISO29022 using a universal testing machine (Instron 5965; Instron Co., Norwood, MA, USA). A 5 kN load cell was

applied in parallel with the bonded surfaces at a crosshead speed of 1mm/min using a knife-edge-shaped tip. The highest breaking force required to break the prepared specimens was measured in newtons (N), and the shear bond strength (SBS) was determined using the formula R = F/A, where "R" is the shear bond strength (MPa), "F" is the force needed to separate the specimen, and "A" is the area of the interface (mm^2), A = πr^2, where "R" is the radius of the tooth base.

2.3.2. Contact Angle

The sessile drop method was used to calculate the contact angle [50]. This was measured on both treated surfaces of zirconia and lithium disilicate discs before the cementation procedure. A digital camera and micro-lens were used to record the contact angle for all specimens, except for specimens in the groups incorporating adhesive application, i.e., the SN, PN, and SPN groups. An LED light with a collimating filter was set up behind the sample. The contact angles were measured at a room temperature of 20 °C. A pipette was used to create a drop of distilled water (10 µL) on the specimen's surface. The water drop photos were recorded 15 s after application and analyzed with Image J software (Version 1.54g) [51]. The procedure was carried out three times for each specimen, and the results were averaged in order to determine the contact angle for each specimen and group.

2.3.3. Scanning Electron Microscopy (SEM)

One sample from each group was evaluated via SEM (FEI, Inspect S50, Czech Republic) with 1000X magnification to assess the surface topography.

2.4. Statistical Analysis

SPSS 23.0 (SPSS Inc., Chicago, IL, USA) was used to conduct statistical analysis. The mean and standard deviation (SD) were used for descriptive statistics. To compare the means of the different groups, a one-way ANOVA test was employed. Tukey's test was also used to determine the statistically significant potential pair means among the groups studied.

3. Results

3.1. Contact Angle Test

The means and standard deviations of the contact angles of lithium disilicate and zirconia materials are presented in Table 3. It was discovered that the plasma group had the lowest contact angle in both lithium disilicate (23.99° ± 5.03) and zirconia (23.35° ± 5.51) materials, with a significant difference compared with all other tested surface treatments ($p < 0.05$). The control group in both ceramics had the highest contact angles, with a significant difference compared with all other tested surface treatments ($p > 0.05$). Figure 3 shows the contact angles of the zirconia/lithium disilicate specimens after different surface treatments.

Table 3. Contact angle of Zirconia & Lithium Disilicate specimens after different surface treatments.

Surface Tx/Materials	Contact Angle (°) Mean/Std Dev	
	Lithium Disilicate	Zirconia
(C) Control Group	53.15 ± 3.61 ^{A}	77.34 ± 6.03 ^{A}
(S) Sandblasting Group	39.92 ± 2.52 ^{B}	52.84 ± 4.51 ^{B}
(P) Plasma Group	23.99 ± 5.03 ^{C}	23.35 ± 5.51 ^{D}
(SP) Sandblasting + Plasma Group	37.70 ± 4.16 ^{B}	35.41 ± 5.13 ^{C}

Levels not connected by same letter per column are significantly different.

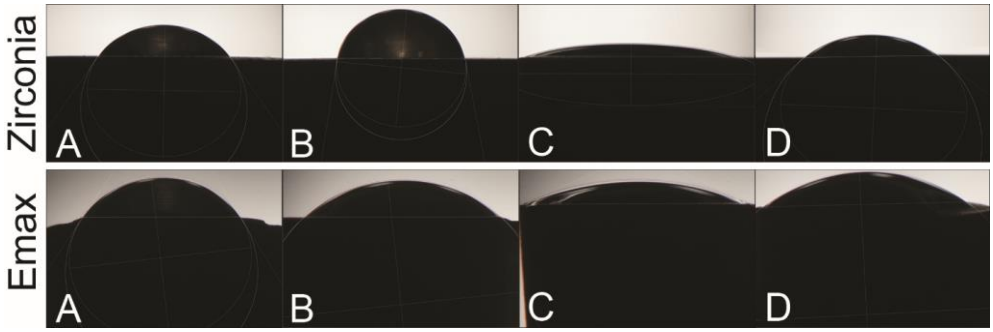


Figure 3. The contact angle of zirconia/lithium disilicate specimens after different surface treatments. (**A**) no treatment; (**B**) sandblasting; (**C**) plasma; and (**D**) plasma and sandblasting.

3.2. Scanning Electron Microscopy (SEM)

The surface topography determined using scanning electron microscopy (SEM) for both ceramics after the different surface treatments is shown in Figure 4. In the zirconia groups, pronounced irregular surfaces were evidenced upon scanning specimens that received either sandblasting only or plasma-and-sandblasting surface treatments. However, irregular and rougher surfaces were observed in sandblasted lithium disilicate-treated surfaces (Figure 4B,D). Plasma-treated surfaces for both zirconia and lithium disilicate revealed virtually no topography changes when compared with the other implemented surface treatments (Figure 4C).

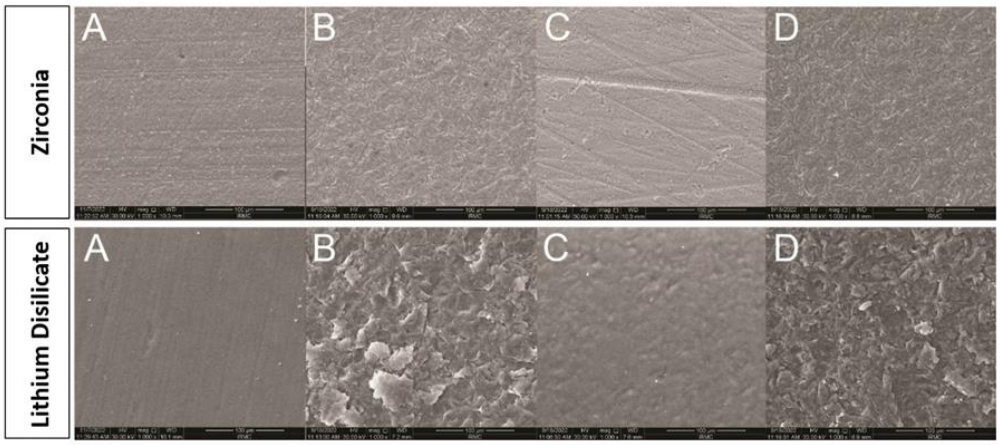


Figure 4. Scanning electron microscopy images of zirconia/lithium disilicate specimens after different surface treatments. (**A**) no treatment; (**B**) sandblasting; (**C**) plasma; and (**D**) plasma and sandblasting.

3.3. Shear Bond Strength Test

Table 4 reveals the means and standard deviations of the shear bond strength test. The untreated control group exhibited the lowest shear bond strength, with a significant difference ($p < 0.05$) compared with the (S), (P), (SP), and (SN) groups. The plasma alone group (P) exhibited the highest shear bond strength value, but this was not statistically significant compared with sandblasting groups (S), (SP), and (SN), with ($p > 0.05$). In terms of the failure mode, all specimens in all groups showed adhesive failure, with no incidence of cohesive or mixed failure detected.

Table 4. Shear bond strength means and standard deviations of all tested groups.

Surface Tx	Mean/Std Dev (MPa)
(C) Control group	6.42 ± 2.13^{C}
(S) Sandblasting group	10.28 ± 2.15^{A}
(P) Plasma group	10.31 ± 1.68^{A}
(SP) Sandblasting + plasma group	10.33 ± 2.35^{A}
(SN) Sandblasting + universal adhesive group	$8.77 \pm 1.85^{A,B}$
(PN) Plasma + universal adhesive group	$6.94 \pm 1.87^{B,C}$
(SPN) Sandblasting + plasma + universal adhesive group	$8.20 \pm 2.44^{B,C}$

Levels not connected by the same letter are significantly different.

4. Discussion

The impact of the handheld plasma device (APPJ) on the wettability, surface topography, and shear bond strength of resin-cemented CAD-on ceramics is a matter of concern. It was hypothesized that plasma surface treatment via APPJ would not affect the wettability or surface topography or provide acceptable shear bond strength between bonded ceramics. The null hypothesis was partially rejected, as the APPJ surface treatment resulted in improved wettability and acceptable shear bond strength while preserving the surface topography of the treated surfaces.

The proposal of the zirconia–lithium disilicate assembly was intended to mimic and support the usage of lithium disilicate as a CAD-on veneering over a zirconia framework with low chipping or delamination incidence [23]. Fusion glass–ceramic was originally recommended for joining the CAD-on, with reported improved strength [21,25]. However, cemented CAD-on over a custom zirconia abutment demonstrated significant loading fracture values when compared with heat-fused CAD-on [26]. Another comparable result was gained upon fatigue and static load failure for both fusion glass–ceramic and the cementation of CAD-On [27]. In the present study, the resin cementation method was selected for joining the CAD-on assembly to avoid residual stresses [28], which alleviates the success rate by suppressing crack propagation while circumventing additional thermal treatment [29]. In addition, the resin cementation method could be applied in the repair of existing delaminated restorations [33]. The usage of resin cementation rather than heat fusion with CAD-on has extended the range of available materials for veneering to include machinable resin-based materials [32].

Studies have shown that untreated ceramic surfaces demonstrate remarkable hydrophilicity, especially zirconia [2,3]. Similarly, in the present study, untreated ceramic surfaces demonstrated significant hydrophilicity, with contact angle values coincident with those in previous studies, for lithium disilicate and zirconia [38]. Within the tested materials, a higher contact angle value was observed with the untreated zirconia surface than the untreated lithium disilicate, thus supporting the previously reported hydrophilicity of zirconia. Sandblasting of both ceramics revealed a progressive reduction in the contact angle measurement with alignment to the aforementioned studies [4,38]. Sandblasting is considered a sensitive technique with a variable outcome due to the numerous incorporated settings, i.e., particle size, pressure, and time [40]. The application of various plasma types has generally been shown to be beneficial in the provision of improved wettability [5,6]. Within the literature, APPJs have been relatively poorly explored, with little documentation on ceramic wettability. Utilizing APPJ devices, a previous study revealed improved wettability with lower contact angle values [19]. In our study, plasma surface treatment alone for both treated ceramic surfaces exhibited the lowest contact angle values among all tested surface treatments, revealing the efficacy of APPJs in providing vastly improved wettability. Additionally, the APPJ treatment revealed enhanced wettability for both tested ceramics in the same manner, providing almost the same contact angle values. The remarkable hydrophilicity of zirconia was inverted to the lower level, with no

difference from plasma-treated lithium disilicate. The combination of sandblasting and plasma surface treatment resulted in significantly better wettability than the sandblasting groups but significantly lower wettability than the plasma groups. This may be due to the reported possible contamination from blasting particles [48].

The non-destructive nature of plasma has been further explained in a study using electron microscopy scanning [19]. Plasma-treated surfaces in our study showed homogenous unchanged surfaces rather than rough or irregular surfaces created by sandblasting. It has been stated that all sandblasting conditions can cause surface deterioration and phase transformation of zirconia to a variable extent, even with low particle size. Such defects could be reflected in the structural durability of zirconia restoration [47,48]. Sandblasting had variable effects on the tested ceramics; lithium disilicate was more affected than zirconia, as evidenced by the prominent surface irregularities revealed via electron microscopy scanning. This result could be attributed to the material properties, with the characteristic improved hardness of zirconia rendering its surface more resistant than high-strength glass–ceramic [3].

The testing of the hypothesized surface-treated zirconia–lithium disilicate interface has only been investigated in terms of shear bond strength, and high clinical survival of the same CAD-on concept was reported in one study [25]. Moreover, the resin–ceramic interface is usually tested under different sandblasting conditions. The results of a ceramic–resin interface investigation showed high shear bond strength [39] but with doubts regarding the preservation of structural durability, especially with blasted zirconia [48]. In the present study, shear bond testing was focused on ceramic interfaces bonded using resin cementation. The plasma surface treatment generated using an APPJ device as a conventional sandblasting surface treatment was significant in producing a high shear bond strength, and the best results were achieved when both plasma and sandblasting were implemented together. The provision of surface reactive species, enhanced wettability, and the cleaning action of plasma application could be attributed to such results [7,8]. The incorporation of a universal adhesive (silane and MDP-containing adhesive) with either sandblasting or plasma surface treatment resulted in a decrease in shear bond strength; moreover, this result was non-significant when combined with sandblasting and significant with plasma application. Such findings may be attributed to the deposition of an extremely thin layer of resin that could subsequently compromise bond strength [52]. Previous studies have challenged the claim of the multipurpose applicability of universal adhesive (silane and MDP-containing adhesive) on indirect ceramic restoration, noting its shortcomings in terms of long-term performance [43].

In this study, it was apparent that APPJ application effectively improved wettability, even in the case of tough hydrophilic surfaces with a low surface treatment effect or structural deterioration, and produced high shear bond strength values. Therefore, the application of APPJ devices could be considered as a non-destructive replacement for the traditional sandblasting surface treatment, coupled with the simplification of plasma application within in-office settings. Compared with other types of plasma, APPJ treatment produced satisfactory results. This renders APPJ treatment an applicable method for ceramic surface treatment or bonding ceramic interfaces rather than relying on laboratory plasma production or destructive mechanical sandblasting. Clinically, it could be feasible to use APPJ devices in treating ceramics within in-office settings. Ceramics are bonded together in CAD-on assembly or even CAD-on repair and in the joining of multiple prosthetic structures over an implant abutment.

As a limitation within testing, further investigations into surface treatments under different settings and/or combinations could be beneficial in the determination of the optimum ceramic treatment. Hence, investigations on variable sandblasting conditions, such as particle size and pressure or other ceramic primers and combinations, are crucial. Ceramic decontamination using APPJs could also be explored, as such contamination is responsible for compromised resin adhesion in indirect ceramic restorations.

In line with mimicking oral conditions, future testing under cyclic loading or aging effects could be relevant to determining long-term performance. Additionally, X-ray diffraction analyses of treated ceramic structures under the tested conditions could also be considered.

5. Conclusions

Within the limitations of this in vitro study, the following conclusions can be drawn. Surface treatments had a pronounced effect on surface characteristics and the shear bond strength between ceramics and the proposed CAD-on assembly. The plasma surface treatment (with handheld jets, APPJs) revealed the advantage of inducing vastly improved wettability while being non-destructive, preserving the surface integrity with no topographical surface alteration. The APPJ surface treatment resulted in significant bond strength when applied separately or combined with sandblasting. However, the incorporation of universal adhesives negatively affected the bonding of the proposed assembly. Lastly, randomized clinical studies are required to validate actual clinical performance.

Author Contributions: Conceptualization H.A., methodology, investigation Z.A.M., O.A.A., F.A.D., M.H., F.A.G. and S.A., and writing, H.A. and M.A.A. All authors have read and agreed to the published version of the manuscript.

Funding: This research received no external funding.

Institutional Review Board Statement: Not applicable.

Informed Consent Statement: Not applicable.

Data Availability Statement: Data are contained within the article.

Conflicts of Interest: The authors declare no conflicts of interest.

References

1. Cha, S.; Park, Y.S. Plasma in dentistry. *Clin. Plasma Med.* **2014**, *2*, 4–10. [CrossRef] [PubMed]
2. Lohbauer, U.; Zipperle, M.; Rischka, K.; Petschelt, A.; Müller, F.A. Hydroxylation of dental zirconia surfaces: Characterization and bonding potential. *J. Biomed. Mater. Res. B Appl. Biomater.* **2008**, *87*, 461–467. [CrossRef] [PubMed]
3. Cavalcanti, A.N.; Foxton, R.M.; Watson, T.F.; Oliveira, M.T.; Giannini, M.; Marchi, G.M. Y-TZP ceramics: Key concepts for clinical application. *Oper. Dent.* **2009**, *34*, 344–351. [CrossRef] [PubMed]
4. Soares, E.J.; de Lima Oliveira, R.F.; Silame, F.D.J.; Tonani-Torrieri, R.; Franca, R.; de CPPires-de-Souza, F. Color stability, translucency, and wettability of a lithium disilicate dental ceramics submitted to different surface treatments. *Int. J. Prosthodont. Restor. Dent.* **2021**, *11*, 4–8.
5. Valverde, G.B.; Coelho, P.G.; Janal, M.N.; Lorenzoni, F.C.; Carvalho, R.M.; Thompson, V.P.; Weltemann, K.-D.; Silva, N.R. Surface characterisation and bonding of Y-TZP following non-thermal plasma treatment. *J. Dent.* **2013**, *41*, 51–59. [CrossRef]
6. Tabari, K.; Hosseinpour, S.; Mohammad-Rahimi, H. The Impact of Plasma Treatment of Cercon® Zirconia Ceramics on Adhesion to Resin Composite Cements and Surface Properties. *J. Lasers Med. Sci.* **2017**, *8* (Suppl. S1), S56–S61. [CrossRef]
7. Heinlin, J.; Isbary, G.; Stolz, W.; Morfill, G.; Landthaler, M.; Shimizu, T.; Steffes, B.; Nosenko, T.; Zimmermann, J.; Karrer, S. Plasma applications in medicine with a special focus on dermatology. *J. Eur. Acad. Dermatol. Venereol.* **2011**, *25*, 1–11. [CrossRef]
8. Silva, N.R.; Coelho, P.G.; Valverde, G.B.; Becker, K.; Ihrke, R.; Quade, A.; Thompson, V.P. Surface characterization of Ti and Y-TZP following non-thermal plasma exposure. *J. Biomed. Mater. Res. B Appl. Biomater.* **2011**, *99*, 199–206. [CrossRef]
9. Dou, S.; Tao, L.; Wang, R.; El Hankari, S.; Chen, R.; Wang, S. Plasma-Assisted Synthesis and Surface Modification of Electrode Materials for Renewable Energy. *Adv. Mater.* **2018**, *30*, e1705850. [CrossRef]
10. Izadjoo, M.; Zack, S.; Kim, H.; Skiba, J. Medical applications of cold atmospheric plasma: State of the science. *J. Wound Care* **2018**, *27* (Suppl. S9), S4–S10. [CrossRef]
11. Domonkos, M.; Tichá, P.; Trejbal, J.; Demo, P. Applications of cold atmospheric pressure plasma technology in medicine, agriculture and food industry. *Appl. Sci.* **2021**, *11*, 4809. [CrossRef]
12. Sakudo, A.; Yagyu, Y.; Onodera, T. Disinfection and Sterilization Using Plasma Technology: Fundamentals and Future Perspectives for Biological Applications. *Int. J. Mol. Sci.* **2019**, *20*, 5216. [CrossRef] [PubMed]
13. Cvelbar, U.; Walsh, J.L.; Černák, M.; de Vries, H.W.; Reuter, S.; Belmonte, T.; Corbella, C.; Miron, C.; Hojnik, N.; Jurov, A.; et al. White paper on the future of plasma science and technology in plastics and textiles. *Plasma Process. Polym.* **2019**, *16*, 1700228. [CrossRef]
14. Kleineidam, B.; Nokhbehsaim, M.; Deschner, J.; Wahl, G. Effect of cold plasma on periodontal wound healing-an in vitro study. *Clin. Oral. Investig.* **2019**, *23*, 1941–1950. [CrossRef]

15. Liu, Y.C.; Hsieh, J.P.; Chen, Y.C.; Kang, L.L.; Hwang, C.S.; Chuang, S.F. Promoting porcelain-zirconia bonding using different atmospheric pressure gas plasmas. *Dent. Mater.* **2018**, *34*, 1188–1198. [CrossRef]
16. Yılmaz Savaş, T.; Akın, C. Effect of nonthermal plasma treatment on surface roughness and bond strength between veneer ceramic and zirconia core. *Int. J. Appl. Ceram. Technol.* **2022**, *19*, 1572–1582. [CrossRef]
17. Korzec, D.; Hoppenthaler, F.; Nettesheim, S. Piezoelectric Direct Discharge: Devices and Applications. *Plasma* **2021**, *4*, 1–41. [CrossRef]
18. Jungbauer, G.; Favaro, L.; Müller, S.; Sculean, A.; Eick, S. The In-Vitro Activity of a Cold Atmospheric Plasma Device Utilizing Ambient Air against Bacteria and Biofilms Associated with Periodontal or Peri-Implant Diseases. *Antibiotics* **2022**, *11*, 752. [CrossRef]
19. Ito, Y.; Okawa, T.; Fujii, T.; Tanaka, M. Influence of plasma treatment on surface properties of zirconia. *J. Osaka Dent. Univ.* **2016**, *50*, 79–84.
20. Alessandretti, R.; Ribeiro, R.; Borba, M.; Bona, A.D. Fracture Load and Failure Mode of CAD-on Ceramic Structures. *Braz. Dent. J.* **2019**, *30*, 380–384. [CrossRef]
21. Alessandretti, R.; Borba, M.; Benetti, P.; Corazza, P.H.; Ribeiro, R.; Della Bona, A. Reliability and mode of failure of bonded monolithic and multilayer ceramics. *Dent. Mater.* **2017**, *33*, 191–197. [CrossRef] [PubMed]
22. Kavut, I.; Külünk, S. Evaluation of the core thickness and resin cement on the fracture strength of zirconia-based multilayer computer-aided design/computer-aided manufacturing ceramic crowns. *Dent. Med. Res.* **2019**, *7*, 16. [CrossRef]
23. Grohmann, P.; Bindl, A.; Hämmerle, C.; Mehl, A.; Sailer, I. Three-unit posterior zirconia-ceramic fixed dental prostheses (FDPs) veneered with layered and milled (CAD-on) veneering ceramics: 1-year follow-up of a randomized controlled clinical trial. *Quintessence Int.* **2015**, *46*, 871–880. [PubMed]
24. Basso, G.R.; Moraes, R.R.; Borba, M.; Duan, Y.; Griggs, J.A.; Della Bona, A. Reliability and failure behavior of CAD-on fixed partial dentures. *Dent. Mater.* **2016**, *32*, 624–630. [CrossRef] [PubMed]
25. Blatz, M.B.; Hariton-Gross, K.; Anadioti, E.; Mante, F.; Zhang, Y.; Saleh, N. Prospective 5-year clinical evaluation of posterior zirconia fixed dental prostheses veneered with milled lithium disilicate (CADon). *J. Esthet. Restor. Dent.* **2022**, *34*, 136–144. [CrossRef]
26. Nossair, S.A.; Aboushelib, M.N.; Morsi, T.S. Fracture and Fatigue Resistance of Cemented versus Fused CAD-on Veneers over Customized Zirconia Implant Abutments. *J. Prosthodont.* **2015**, *24*, 543–548. [CrossRef]
27. Sasany, R.; Yilmaz, B. Marginal discrepancy and fracture load of thermomechanically fatigued crowns fabricated with different CAD-CAM techniques. *J. Prosthodont.* **2022**, *32*, 602–607. [CrossRef]
28. Costa, A.K.; Borges, A.L.; Fleming, G.J.; Addison, O. The strength of sintered and adhesively bonded zirconia/veneer-ceramic bilayers. *J. Dent.* **2014**, *42*, 1269–1276. [CrossRef]
29. Lee, J.J.-W.; Lloyd, I.K.; Chai, H.; Jung, Y.-G.; Lawn, B.R. Arrest, deflection, penetration and reinitiation of cracks in brittle layers across adhesive interlayers. *Acta Mater.* **2007**, *55*, 5859–5866. [CrossRef]
30. Schmitter, M.; Mueller, D.; Rues, S. Chipping behaviour of all-ceramic crowns with zirconia framework and CAD/CAM manufactured veneer. *J. Dent.* **2012**, *40*, 154–162. [CrossRef]
31. Schmitter, M.; Mueller, D.; Rues, S. In vitro chipping behaviour of all-ceramic crowns with a zirconia framework and feldspathic veneering: Comparison of CAD/CAM-produced veneer with manually layered veneer. *J. Oral. Rehabil.* **2013**, *40*, 519–525. [CrossRef] [PubMed]
32. Wiedenmann, F.; Klören, M.; Edelhoff, D.; Stawarczyk, B. Bond strength of CAD-CAM and conventional veneering materials to different frameworks. *J. Prosthet. Dent.* **2021**, *125*, 664–673. [CrossRef] [PubMed]
33. Saeidi Pour, R.; Edelhoff, D.; Rafael, C.F.; Prandtner, O.; Frei, S.; Maziero Volpato, C.A.; Liebermann, A. Combining Esthetic Layering and Lithium Disilicate Sintering Technique on Zirconia Frameworks: A Veneering Option to Prevent Ceramic Chipping. *Int. J. Periodontics Restor. Dent.* **2017**, *37*, 561–569. [CrossRef] [PubMed]
34. Fathpour, K.; Nili Ahmadabadi, M.; Atash, R.; Fathi, A.H. Effect of Different Surface Treatment Methods on the Shear Bond Strength of Resin Composite/Zirconia for Intra-oral Repair of Zirconia Restorations. *Eur. J. Dent.* **2022**, *17*, 809–817. [CrossRef]
35. Al-Hmadi, S.; Erol, F.; Guven Celik, M. Shear bond strengths of five porcelain repair systems to zirconia infrastructures. *Eur. Oral. Res.* **2022**, *56*, 55–60. [CrossRef]
36. Malysa, A.; Wezgowiec, J.; Orzeszek, S.; Florjanski, W.; Zietek, M.; Wieckiewicz, M. Effect of Different Surface Treatment Methods on Bond Strength of Dental Ceramics to Dental Hard Tissues: A Systematic Review. *Molecules* **2021**, *26*, 1223. [CrossRef]
37. Alagiriswamy, G.; Krishnan, C.S.; Ramakrishnan, H.; Jayakrishnakumar, S.K.; Mahadevan, V.; Azhagarasan, N.S. Surface Characteristics and Bioactivity of Zirconia (Y-TZP) with Different Surface Treatments. *J. Pharm. Bioallied Sci.* **2020**, *12* (Suppl. S1), S114–S123.
38. Li, W.; Ding, Q.; Sun, F.; Liu, B.; Yuan, F.; Zhang, L.; Bao, R.; Gu, J.; Lin, Y. Fatigue behavior of zirconia with microgrooved surfaces produced using femtosecond laser. *Lasers Med. Sci.* **2023**, *38*, 33. [CrossRef]
39. Seo, S.H.; Kim, J.E.; Nam, N.E.; Moon, H.S. Effect of air abrasion, acid etching, and aging on the shear bond strength with resin cement to 3Y-TZP zirconia. *J. Mech. Behav. Biomed. Mater.* **2022**, *134*, 105348. [CrossRef]
40. Su, N.; Yue, L.; Liao, Y.; Liu, W.; Zhang, H.; Li, X.; Wang, H.; Shen, J. The effect of various sandblasting conditions on surface changes of dental zirconia and shear bond strength between zirconia core and indirect composite resin. *J. Adv. Prosthodont.* **2015**, *7*, 214–223. [CrossRef]

41. Borges, G.A.; Sophr, A.M.; de Goes, M.F.; Sobrinho, L.C.; Chan, D.C. Effect of etching and airborne particle abrasion on the microstructure of different dental ceramics. *J. Prosthet. Dent.* **2003**, *89*, 479–488. [CrossRef] [PubMed]
42. Della Bona, A.; Borba, M.; Benetti, P.; Pecho, O.E.; Alessandretti, R.; Mosele, J.C.; Mores, R.T. Adhesion to dental ceramics. *Curr. Oral. Health Rep.* **2014**, *1*, 232–238. [CrossRef]
43. Nagarkar, S.; Theis-Mahon, N.; Perdigão, J. Universal dental adhesives: Current status, laboratory testing, and clinical performance. *J. Biomed. Mater. Res. B Appl. Biomater.* **2019**, *107*, 2121–2131. [CrossRef] [PubMed]
44. Zarone, F.; Di Mauro, M.I.; Ausiello, P.; Ruggiero, G.; Sorrentino, R. Current status on lithium disilicate and zirconia: A narrative review. *BMC Oral. Health* **2019**, *19*, 134. [CrossRef]
45. Yilmaz, A.D.; Okutan, Y. Effect of air-abrasion at pre- and/or post-sintered stage and hydrothermal aging on surface roughness, phase transformation, and flexural strength of multilayered monolithic zirconia. *J. Biomed. Mater. Res. B Appl. Biomater.* **2021**, *109*, 606–616. [CrossRef]
46. Yamaguchi, H.; Ino, S.; Hamano, N.; Okada, S.; Teranaka, T. Examination of bond strength and mechanical properties of Y-TZP zirconia ceramics with different surface modifications. *Dent. Mater. J.* **2012**, *31*, 472–480. [CrossRef]
47. Campos, F.; Souza, R.O.; Bottino, M.A.; Özcan, M. Fracture Strength, Failure Types, and Weibull Characteristics of Three-Unit Zirconia Fixed Dental Prostheses After Cyclic Loading: Effects of Veneering and Air-Abrasion Protocols. *Int. J. Periodontics Restor. Dent.* **2016**, *36*, 901–908. [CrossRef]
48. Strasser, T.; Preis, V.; Behr, M.; Rosentritt, M. Roughness, surface energy, and superficial damages of CAD/CAM materials after surface treatment. *Clin. Oral. Investig.* **2018**, *22*, 2787–2797. [CrossRef]
49. International Organization for Standardization. *Dentistry, Adhesion, Notched-Edge Shear Bond Strength Test*; International Organization for Standardization: Geneva, Switzerland, 2013. Available online: https://www.iso.org/standard/45285.html (accessed on 3 September 2024).
50. Noro, A.; Kaneko, M.; Murata, I.; Yoshinari, M. Influence of surface topography and surface physicochemistry on wettability of zirconia (tetragonal zirconia polycrystal). *J. Biomed. Mater. Res. B Appl. Biomater.* **2013**, *101*, 355–363. [CrossRef]
51. Schneider, C.A.; Rasband, W.S.; Eliceiri, K.W. NIH Image to ImageJ: 25 years of image analysis. *Nat. Methods* **2012**, *9*, 671–675. [CrossRef]
52. Strazzi-Sahyon, H.B.; Rocha, E.P.; AssunÇÃo, W.G.; Dos Santos, P.H. Role of adhesive systems on the luting interface's thickness of ceramic laminate veneers. *Braz. Oral. Res.* **2020**, *34*, e063. [CrossRef]

Disclaimer/Publisher's Note: The statements, opinions and data contained in all publications are solely those of the individual author(s) and contributor(s) and not of MDPI and/or the editor(s). MDPI and/or the editor(s) disclaim responsibility for any injury to people or property resulting from any ideas, methods, instructions or products referred to in the content.